Peristaltic Motion of a Carreau Fluid in an Asymmetric Channel with Partial Slip

K. Rajanikanth[1], S. Sreenadh[2], A. Ebaid[3]
[1] Department of Mathematics, GDC, Mylavaram 512320, AP, India
[2] Department of Mathematics, Sri Venkateswara University, Tirupati 517 502, AP, India
[3] Department of Mathematics, Facultyof Science, Tabuk University, P.O. Box 741,Tabuk 71491,Saudi Arabia

***Abstract*— The peristaltic motion of a Carreau fluid in an asymmetric channel with partial slip is studied under long wave length and low Reynolds number assumptions which are also used to solve the problem. Applying perturbation technique, the expressions for stream function, axial velocity, axial pressure gradient, pressure rise, shear stress and frictional forces have been obtained. The effects of various emerging parameters on the flow characteristics are shown and discussed with the help of graphs. The pumping is examined for different wave forms. The results of the current paper reveal that the size of the trapping bolus increases by Carreau fluid (n=0.398) to Newtonian fluid (n=1).**

Keywords*— peristaltic transport, asymmetric channel, Weissenberg number, partial slip, shear stress, trapping, different wave forms.

I. INTRODUCTION

The study of peristaltic transport in fluid mechanics has been carried out by many researchers to look for its implication in the biological sciences in general and in biomechanics in particular. The peristaltic flow occurs due to the contraction and expansion of a progressive wave propagating along the length of a distensible tube containing fluid. Peristaltic wave causing transportation of the fluid through muscular tube is indeed an important biological mechanism responsible for various physiological functions of many organs of the human body. Such mechanism may be involved in urine transport from kidney to bladder through the ureter, swallowing foods through the esophagus, the transport of spermatozoa in the cervical canal, the movement of chyme in small intestines and in the transport of bile. Such a wide occurrence of peristaltic motion should not be surprising at all since it results physiologically from neuro-muscular properties of any tubular smooth muscle.

Most of the previous works in the literature deals with the peristaltic flow in a symmetric channel or tube. Due attention has not been given to the peristaltic mechanism in an asymmetric channel. Recently, physiologists observed that myometrial contractions may occur in both symmetric and asymmetric directions. Eytan and Elad [1] have presented a mathematical model of wall induced peristaltic fluid flow in a two-dimensional channel with wave trains having a phase difference moving independently on the upper and lower walls to stimulate intra-uterine fluid motion in a sagittal cross –section of the uterus. In another paper, Eytan et al. [2] reported that the width of the sagittal cross-section of the uterine cavity increases towards the fundus and the cavity is not fully occluded during the contractions. Mishra and Rao [3] discussed the peristaltic motion of viscous fluid in a two-dimensional asymmetric channel under long wavelength assumption. Rao and Mishra [4] also analyzed the curvature effects on peristaltic transport in an asymmetric channel. Hayat et al [5] studied **p**eristaltic flow of a micropolar fluid in a channel with different wave forms. Vajravelu et al. [6] investigated **the p**eristaltic transport of a Casson fluid in contact with a Newtonian **f**luid in a circular **t**ube with permeable wall. Ali and Hayat **[**7] made a detailed study as the peristaltic motion of a Carreau fluid in an asymmetric channel with impermeable walls. Vajravelu et al [8] studied **p**eristaltic transport of a Williamson fluid in asymmetric channels with permeable walls. Nadeem [9] found **h**eat transfer in a peristaltic flow of MHD fluid with partial slip. Hayat [10] investigated **the** influence of partial slip on the peristaltic flow in a porous medium. Since many biological systems such as blood vessels contain a tissue layer it will be interesting to study peristaltic transport of a biofluid through asymmetric channel with partial slip. Prasanna et al [11] examined the peristaltic transport of non-Newtonian fluid in a diverging tube with different wave forms as the peristaltic wave form in living organisms is not known. This method has already been used for the solutions of several other problems [12–15].

The main objective of **the** present investigation is to put forward the analysis of peristaltic flow of a Carreau fluid in an asymmetric channel. The Carreau fluid model is a four parameter model and has useful properties of a truncated power law model that does not have a discontinuous first derivative. The relevant equations for the fluid under consideration have been first modeled and then solved. The assumption for the solution is that wavelength of the peristaltic wave is long. A regular perturbation technique is employed to solve the present problem and solutions are expanded in a power of small Weissenberg number. The analysis is made for the stream function, axial pressure gradient and pressure drop over a wavelength. The influence of emerging parameters is shown on pumping, pressure gradient and trapping.

II. MATHEMATICAL FORMULATION

Let us consider the peristaltic transport of an incompressible Carreau fluid in a two–dimensional channel of width $d_1 + d_2$ (Fig. 1). The flow is generated by sinusoidal wave trains propagating with constant speed c along the permeable walls of the channel. The geometry of the wall surfaces is defined as

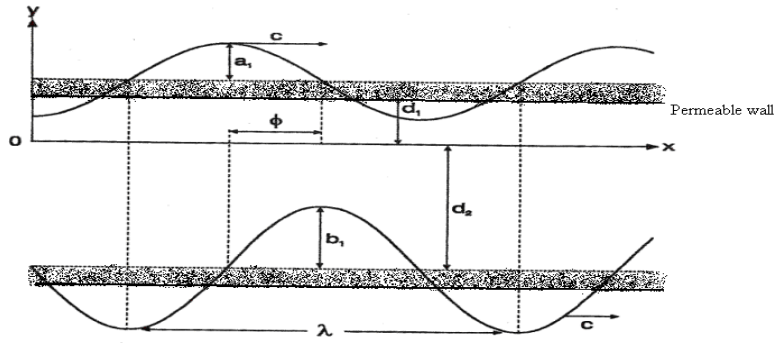

Fig. 1: Schematic diagram of a two-dimensional asymmetric channel

$$h_1(\bar{X},\bar{t}) = \bar{d}_1 + \bar{a}_1 \cos\left[\frac{2\pi}{\lambda}(\bar{X} - ct)\right] \quad \text{....} \quad \text{upper wall,} \tag{1}$$

$$h_2(\bar{X},\bar{t}) = -\bar{d}_2 - \bar{a}_2 \cos\left[\frac{2\pi}{\lambda}(\bar{X} - ct) + \phi\right] \quad \text{.....} \quad \text{lower wall.} \tag{2}$$

in which $\bar{a}_1$ and $\bar{b}_1$ are the amplitudes of the waves, λ is the wave length, c is the wave speed, ϕ $(0 \le \phi \le \pi)$ is the phase difference, $\bar{X}$ and $\bar{Y}$ are the rectangular coordinates with $\bar{X}$ measured along the axis of the channel and $\bar{Y}$ **is** perpendicular to $\bar{X}$. Let $(\bar{U},\bar{V})$ be the velocity components in fixed frame of reference $(\bar{X},\bar{Y})$. It should be noted that $\phi = 0$ corresponding to symmetric channel with waves out of phase and for $\phi = \pi$ the waves are in phase. Furthermore, $\bar{a}_1,\ \bar{a}_2,\ \bar{d}_1,\ \bar{d}_2$ and ϕ satisfy the condition

$$\bar{a}_1^{\,2} + \bar{b}_1^{\,2} + 2\bar{a}_1\bar{b}_1 \cos\phi \le \left(\bar{d}_1 + \bar{d}_2\right)^2 \quad . \tag{3}$$

III. EQUATIONS OF MOTION

The constitutive equation for a Carreau fluid is (Ref. [7])

$$\bar{\tau} = -\left[\eta_\infty + (\eta_0 - \eta_\infty)\left(1 + (\Gamma\bar{\dot{\gamma}})^2\right)^{\frac{n-1}{2}}\right]\bar{\dot{\gamma}}, \tag{4}$$

where τ is the extra stress tensor, η_∞ is the infinite shear rate viscosity, η_0 is the zero shear-rate viscosity, Γ is the time constant, *n* is the dimensionless power law index and $\dot{\gamma}$ is defined as

$$\bar{\dot{\gamma}} = \sqrt{\frac{1}{2}\sum_i\sum_j \bar{\dot{\gamma}}_{ij}\bar{\dot{\gamma}}_{ji}} = \sqrt{\frac{1}{2}\Pi} \quad . \tag{5}$$

here Π is the second invariant of strain- rate tensor. We consider in the constitutive Eq. (4) the case for which $\eta_\infty = 0$, and so we can write

$$\bar{\tau} = -\eta_0\left[1 + (\Gamma\bar{\dot{\gamma}})^2\right]^{\frac{n-1}{2}}\bar{\dot{\gamma}}. \tag{6}$$

The above model reduces to Newtonian Model for *n*=1 or $\Gamma = 0$.

The flow is unsteady in the laboratory frame $(\bar{X},\bar{Y})$. However, if observed in a moving coordinate system with the wave speed *c* (wave frame) $(\bar{x},\bar{y})$ it can be treated as steady. The coordinates and velocities in the two frames are

$$\bar{x} = \bar{X} - c\bar{t},\ \ \bar{y} = \bar{Y},\ \bar{u}(\bar{x},\bar{y}) = \bar{U} - c,\ \bar{v}(\bar{x},\bar{y}) = \bar{V}, \tag{7}$$

where $\bar{u}$ and $\bar{v}$ indicate the velocity components in the wave frame. The equations the following of a Carreau fluid are given by

$$\frac{\partial\bar{u}}{\partial\bar{x}} + \frac{\partial\bar{v}}{\partial\bar{y}} = 0, \tag{8}$$

$$\rho\left(\bar{u}\frac{\partial}{\partial\bar{x}} + \bar{v}\frac{\partial}{\partial\bar{y}}\right)\bar{u} = -\frac{\partial\bar{p}}{\partial\bar{x}} - \frac{\partial\bar{\tau}_{\bar{x}\bar{x}}}{\partial\bar{x}} - \frac{\partial\tau_{\bar{x}\bar{y}}}{\partial\bar{y}} \tag{9}$$

$$\rho\left(\bar{u}\frac{\partial}{\partial\bar{x}} + \bar{v}\frac{\partial}{\partial\bar{y}}\right)\bar{v} = -\frac{\partial\bar{p}}{\partial\bar{y}} - \frac{\partial\bar{\tau}_{\bar{x}\bar{y}}}{\partial\bar{x}} - \frac{\partial\tau_{\bar{y}\bar{y}}}{\partial\bar{y}}. \tag{10}$$

The following non-dimension quantities are also defined

$$\bar{x}=\frac{\bar{x}}{\lambda},\ y=\frac{\bar{y}}{\bar{d}_1},\ u=\frac{\bar{u}}{c},\ v=\frac{\bar{v}}{c},\ t=\frac{c}{\lambda}\bar{t},\ h_1=\frac{\bar{h}_1}{\bar{d}_1}, a=\frac{\bar{a}_1}{\bar{d}_1}, b=\frac{\bar{a}_2}{\bar{d}_1},\ d=\frac{\bar{d}_2}{\bar{d}_1},\ \dot{\gamma}=\frac{\bar{\dot{\gamma}}\bar{d}_1}{c}, \delta=\frac{\bar{d}_1}{\lambda},$$

$$h_2=\frac{\bar{h}_2}{\bar{d}_1}, \tau_{xx}=\frac{\lambda}{\eta_0 c}\bar{\tau}_{\bar{x}\bar{x}}, \tau_{xy}=\frac{\bar{d}_1}{\eta_0 c}\bar{\tau}_{\bar{x}\bar{y}}, \tau_{yy}=\frac{\bar{d}_1}{\eta_0 c}\bar{\tau}_{\bar{y}\bar{y}}, We=\frac{\Gamma c}{d_1}, p=\frac{\bar{d}_1^{\,2}}{c\lambda\eta_0}\bar{p}, \mathrm{Re}=\frac{\rho c\bar{d}_1}{\eta_0}, Da=\frac{k}{d_1^2}. \tag{11}$$

and the stream function $\psi(x,y)$ is defined by

$$u=\frac{\partial\psi}{\partial y}, v=-\delta\frac{\partial\psi}{\partial x}. \tag{12}$$

Using the above non-dimensional quantities given in Eqs. (8) - (10), the resulting equations in terms of stream function can be written as

$$\delta\,\mathrm{Re}\left[\left(\frac{\partial\psi}{\partial y}\frac{\partial}{\partial x}-\frac{\partial\psi}{\partial x}\frac{\partial}{\partial y}\right)\frac{\partial\psi}{\partial y}\right]=-\frac{\partial p}{\partial x}-\frac{\delta^2}{2}\frac{\partial\tau_{xx}}{\partial x}-\frac{\partial\tau_{xy}}{\partial y}, \tag{13}$$

$$-\delta^3\,\mathrm{Re}\left[\left(\frac{\partial\psi}{\partial y}\frac{\partial}{\partial x}-\frac{\partial\psi}{\partial x}\frac{\partial}{\partial y}\right)\frac{\partial\psi}{\partial x}\right]=-\frac{\partial p}{\partial y}-\delta^2\frac{\partial\tau_{xy}}{\partial x}-\delta\frac{\partial\tau_{yy}}{\partial y}. \tag{14}$$

where

$$\tau_{xx}=-2\left[1+\frac{(n-1)}{2}We^2\dot{\gamma}^2\right]\frac{\partial^2\psi}{\partial x\partial y}, \tag{15}$$

$$\tau_{xy}=-\left[1+\frac{(n-1)}{2}We^2\dot{\gamma}^2\right]\left(\frac{\partial^2\psi}{\partial y^2}-\delta^2\frac{\partial^2\psi}{\partial x^2}\right), \tag{16}$$

$$\tau_{yy}=2\delta\left[1+\frac{(n-1)}{2}We^2\dot{\gamma}^2\right]\frac{\partial^2\psi}{\partial x\partial y}, \tag{17}$$

$$\dot{\gamma}=\left[2\delta^2\left(\frac{\partial^2\psi}{\partial x\partial y}\right)^2+\left(\frac{\partial^2\psi}{\partial y^2}-\delta^2\frac{\partial^2\psi}{\partial x^2}\right)+2\delta^2\left(\frac{\partial^2\psi}{\partial x\partial y}\right)^2\right]^{\frac{1}{2}}. \tag{18}$$

and δ, *Re* and *We* are the wave, Reynolds and Weisssenberg numbers, respectively. Under the assumptions of long wavelength and low Reynolds number**,** Eqs (13) - (14) after using Eq. (16) become

$$\frac{\partial p}{\partial x}=\frac{\partial}{\partial y}\left[1+\frac{(n-1)}{2}We^2\left(\frac{\partial^2\psi}{\partial y^2}\right)^2\right]\frac{\partial^2\psi}{\partial y^2}, \tag{19}$$

$$\frac{\partial p}{\partial y}=0. \tag{20}$$

On eliminating the pressure *p* from Eqs. (19) - (20), we finally get

$$\frac{\partial^2}{\partial y^2}\left[1+\frac{(n-1)}{2}We^2\left(\frac{\partial^2\psi}{\partial y^2}\right)^2\right]\frac{\partial^2\psi}{\partial y^2}=0. \tag{21}$$

IV. RATE OF VOLUME FLOW AND BOUNDARY CONDITIONS

In laboratory frame, the dimensional volume flow rate is

$$Q=\int_{\bar{h}_2(\bar{X},\bar{t})}^{\bar{h}_1(\bar{X},t)}\bar{U}\left(\bar{X},\bar{Y},\bar{t}\right)d\bar{Y}. \tag{22}$$

in which $\bar{h}_1$ and $\bar{h}_2$ are functions of $\bar{X}$ and $\bar{t}$, the above expression in the wave frame becomes

$$q=\int_{\bar{h}_2(\bar{x})}^{\bar{h}_1(\bar{x})}\bar{u}(\bar{x},\bar{y})d\bar{y}, \tag{23}$$

where $\bar{h}_1$ and $\bar{h}_2$ are only functions of $\bar{x}$, from Eqs. (7), (22) and (23) we can write

$$Q=q+c\bar{h}_1(\bar{x})-c\bar{h}_2(\bar{x}). \tag{24}$$

The time- averaged flow over a period *T* at a fixed position $\bar{X}$ is given as

$$\bar{Q}=\frac{1}{T}\int_0^T Qdt. \tag{25}$$

Where

$$\bar{Q} = \frac{\theta}{c\bar{d}_1}, \quad q = \frac{F}{c\bar{d}_1},$$

(26)

$$F = \int_{h_2(x)}^{h1(x)} \frac{\partial \psi}{\partial y} dy = \psi(h_1(x)) - \psi(h_2(x)) \tag{27}$$

Here, $h_1(x)$ and $h_2(x)$ represent the dimensionless form of the surfaces of the peristaltic walls

$$h_1(x) = 1 + a\cos 2\pi x, \tag{28}$$

$$h_2(x) = -d - b\cos(2\pi x + \phi). \tag{29}$$

On substituting (24) into (25) and performing the integration, we obtain

$$\theta = F + c\bar{d}_1 + c\bar{d}_2, \tag{30}$$

Inserting Eq. (26) into Eq. (30), yields

$$\bar{Q} = q + 1 + d. \tag{31}$$

In the wave frame, the boundary conditions in terms of streams function ψ are (Ref. [10])

$$\psi = \frac{q}{2} at\ y = h_1(x), \tag{32}$$

$$\psi = \frac{-q}{2} at\ y = h_2(x), \tag{33}$$

$$\frac{\partial \psi}{\partial y} + \beta \frac{\partial^2 \psi}{\partial y^2} = -1\ at\ y = h_1(x), \tag{34}$$

$$\frac{\partial \psi}{\partial y} - \beta \frac{\partial^2 \psi}{\partial y^2} = -1\ at\ y = h_2(x). \tag{35}$$

V. PERTURBATION SOLUTION

For perturbation solution, we expand ψ, q and p as

$$\psi = \psi_0 + We^2\psi_1 + O(We^4), \tag{36}$$

$$q = q_0 + We^2 q_1 + O(We^4), \tag{37}$$

$$p = p_0 + We^2 p_1 + O(We^4). \tag{38}$$

System of order We^0:

$$\frac{\partial^4 \psi_0}{\partial y^4} = 0, \tag{39}$$

$$\frac{\partial p_0}{\partial x} = \frac{\partial^3 \psi_0}{\partial y^3}, \tag{40}$$

$$\psi_0 = \frac{q_0}{2} at\ y = h_1(x), \tag{41}$$

$$\psi_0 = \frac{-q_0}{2} at\ y = h_2(x), \tag{42}$$

$$\frac{\partial \psi_0}{\partial y} + \beta \frac{\partial^2 \psi_0}{\partial y^2} = -1\ at\ y = h_1(x), \tag{43}$$

$$\frac{\partial \psi_0}{\partial y} - \beta \frac{\partial^2 \psi_0}{\partial y^2} = -1\ at\ y = h_2(x). \tag{44}$$

System of order We^2

$$(\underline{\text{replace } \psi \text{ by } \psi_1})\ \frac{\partial^4 \psi}{\partial y^4} + \frac{(n-1)}{2} \frac{\partial^2}{\partial y^2} \left[\left(\frac{\partial^2 \psi_0}{\partial y^2} \right)^3 \right] = 0, \tag{45}$$

$$\frac{\partial p_1}{\partial y} = \frac{\partial^3 \psi_1}{\partial y^3} + \frac{(n-1)}{2} \frac{\partial}{\partial y} \left[\left(\frac{\partial^2 \psi_0}{\partial y^2} \right)^3 \right]. \tag{46}$$

$$\psi_1 = \frac{q_1}{2} at\ y = h_1(x), \tag{47}$$

$$\psi_1 = \frac{-q_1}{2} \text{ at } y = h_2(x), \tag{48}$$

$$\frac{\partial \psi_1}{\partial y} + \beta \frac{\partial^2 \psi_1}{\partial y^2} = 0 \text{ at } y = h_1(x), \tag{49}$$

$$\frac{\partial \psi_1}{\partial y} - \beta \frac{\partial^2 \psi_1}{\partial y^2} = 0 \text{ at } y = h_2(x) \quad . \tag{50}$$

A. *Solution for system of order* We^0 *:*

Solving Eq. (39) and then using the boundary conditions given in (41) - (44) we have

$$\psi_0 = A_1 \frac{y^3}{3!} + A_2 \frac{y^2}{2!} + A_3 y + A_4 \tag{51}$$

where

$$A_1 = \frac{-12(q_0 + h_1 - h_2)}{(h_1 - h_2)^2 (h_1 - h_2 + 6\beta)},$$

$$A_2 = \frac{6(q_0 + h_1 - h_2)(h_1 + h_2)}{(h_1 - h_2)^2 [h_1 - h_2 + 6\beta]},$$

$$A_3 = -1 + \frac{6(q_0 + h_1 - h_2)[(h_1 - h_2) - h_1 h_2]}{(h_1 - h_2)^2 [h_1 - h_2 + 6\beta]},$$

$$A_4 = \left(\frac{q_0}{2} + h_1\right) + \frac{(q_0 + h_1 - h_2)[6\beta h_1 (h_1 - h_2) - h_1^3 + 3h_1^2 h_2]}{(h_1 - h_2)^2 [h_1 - h_2 + 6\beta]}.$$

The expressions for the axial pressure gradient at this order is

$$\frac{\partial p_0}{\partial x} = \frac{-12(q_0 + h_1 - h_2)}{(h_1 - h_2)^2 (h_1 - h_2 + 6\beta)}. \tag{52}$$

Integrating Eq. (52) over per wavelength we get

$$\Delta P_{\lambda 0} = \int_0^1 \frac{dp_0}{dx} dx \tag{53}$$

B. *Solution for system of order* We^1 *(the index should be 2):*

Substituting the zeroth-order solution (51) and Eq. (45) and solving the resulting system along with the corresponding boundary conditions we obtain

$$\psi_1 = C_1 \frac{y^3}{3!} + C_2 \frac{y^2}{2!} + C_3 y + C_4 + L_{11} y^5 + L_{12} y^4. \tag{54}$$

where

$$C_1 = \frac{-12q_1 + L_{17}(h_1 - h_2)}{(h_1 - h_2)^2 [h_1 - h_2 + 6\beta]},$$

$$C_2 = \frac{6q_1 + L_{18}}{(h_1 - h_2)^2 [h_1 - h_2 + 6\beta]},$$

$$C_3 = \frac{6q_1 (h_2^2 - h_2 - 2\beta h_2 + \beta) + L_{19}}{(h_1 - h_2)^2 [h_1 - h_2 + 6\beta]},$$

$$C_4 = -\frac{q_1}{2} + \frac{q_1 (2h_1^3 - 3h_1^2) - 6h_1 (h_2^2 - h_2 - 2\beta h_1 + \beta) - L_{20}}{(h_1 - h_2)^2 [h_1 - h_2 + 6\beta]}.$$

$$L_{11} = \frac{-(n-1)c_1^3}{40},$$

$$L_{12} = \frac{-(n-1)c_1^2 c_2}{8},$$

$$L_{13} = 5L_{11} h_1^3 (h_1 + 4\beta) + 4L_{12} h_1^2 (h_1 + 3\beta),$$

$$L_{14} = 5L_{11} h_2^3 (h_2 - 4\beta) + 4L_{12} h_2^2 (h_2 - 3\beta),$$

$$L_{15}=\frac{L_{14}-L_{13}}{(h_1-h_2+2\beta)},$$

$$L_{16}=\frac{1}{(h_1-h_2)}\left[L_{11}\left(h_1^5-h_2^5\right)+L_{12}\left(h_1^4-h_2^4\right)-L_{13}\left(h_1-h_2\right)\right],$$

$$L_{17}=6L_{15}\left(h_2-h_1-2\beta\right)+12L_{16},$$

$$L_{18}=L_{15}\left(h_1-h_2\right)^2\left[h_1-h_2+6\beta\right]-\frac{1}{2}L_{17}\left(h_1-h_2\right),$$

$$L_{19}=\frac{1}{2}L_{17}(h_1-h_2)\left(h_2^2-2\beta h_2\right)+L_{18}\left(h_2-\beta\right)+L_{14}\left(h_1-h_2\right)^2\left(h_1-h_2+6\beta\right),$$

$$L_{20}=\frac{1}{6}L_{17}h_1^3\left(h_1-h_2\right)+\frac{1}{2}L_{18}h_1^2-L_{19}h_1+\left(L_{11}h_1^5+L_{12}h_1\right)\left(h_1-h_2\right)^2\left(h_1-h_2+6\beta\right).$$

The axial pressure gradient is given by

$$\frac{dp_1}{dx}=\frac{-12q_1+L_{17}(h_1-h_2)}{\left(h_1-h_2\right)^2\left(h_1-h_2+6\beta\right)}-\frac{648(n-1)\left(q_0+h_1-h_2\right)^3\left(h_1+h_2\right)^2}{\left(h_1-h_2\right)^6\left(h_1-h_2+6\beta\right)^3}.$$

(55)

Integrating Eq. (55) over are wavelength we get the pressure as

$$\Delta P_{\lambda 1}=\int_0^1\frac{dp_1}{dx}dx. \tag{56}$$

The perturbation series solution up to second order for stream function ψ, velocity u, pressure gradient *dp/dx* and pressure rise ΔP_λ may be summarized as

$$\psi=A_1\frac{y^3}{3!}+A_2\frac{y^2}{2!}+A_3y+A_4+We^2\left(C_1\frac{y^3}{3!}+C_2\frac{y^2}{2!}+C_3y+C_4+L_{11}y^5+L_{12}y^4\right). \tag{57}$$

$$u=A_1\frac{y^2}{2!}+A_2y+A_3+We^2\left(C_1\frac{y^2}{2!}+C_2y+C_3+5L_{11}y^4+4L_{12}y^3\right). \tag{58}$$

$$\frac{dp}{dx}=\frac{dp_0}{dx}+We^2\frac{dp_1}{dx}, \tag{59}$$

$$\Delta P_\lambda=\Delta P_{\lambda 0}+We^2\Delta P_{\lambda 1} \tag{60}$$

The non-dimensional shear stress of the channel reduces to

$$\tau_{xy}=-\left[\frac{6\left(q_0+h_1-h_2\right)\left(h_1+h_2-2y\right)}{\left(h_1-h_2\right)^2\left(h_1-h_2+6\beta\right)}+We^2\left(\frac{108(n-1)\left(q_0+h_1-h_2\right)^3\left(h_1+h_2-2y\right)^3}{\left(h_1-h_2\right)^6\left(h_1-h_2+6\beta\right)^3}-\frac{6q_1(1-y)+L_{17}y+L_{18}}{\left(h_1-h_2\right)^2\left(h_1-h_2+6\beta\right)}+20L_{11}y^3+12L_{12}y^2\right)\right]. \tag{61}$$

By neglecting the terms of orders greater than O (We^2), the results given by Eqs.(57)–(61) are therefore expressed up to We^2. The frictional force, at y= h_1 and y= h_2 denoted by

$$F_{\lambda 1}=\int_0^1-h_1{}^2\left(\frac{dp}{dx}\right)dx, \tag{62}$$

$$F_{\lambda 2}=\int_0^1-h_2{}^2\left(\frac{dp}{dx}\right)dx. \tag{63}$$

VI. RESULTS AND DISCUSSION:

In this section, the results are presented and discussed for different physical quantities of interest. The pressure rise is an important physical measure in the peristaltic mechanism. The perturbation method on Weissenberg number restricted us for choosing the parameters for Carreau fluid such that Weissenberg number is less than one. According to Bird et al. [16] the values of various parameters for Carreau fluid are: n = 0.398, 0.496. Fig. 2 is plotted for dimensionless pressure rise ΔP_λ versus the dimensionless flow rate $\bar{Q}$ to the effects of partial slip β, Weissenberg number *We*, amplitude ratio Φ. The pumping regions are peristaltic pumping ($\bar{Q}>0$, $\Delta P_\lambda>0$), augment pumping ($\bar{Q}<0$, $\Delta P_\lambda<0$), retrograde pumping ($\bar{Q}<0$, $\Delta P_\lambda>0$), copumping ($\bar{Q}>0$, $\Delta P_\lambda<0$) and free pumping ($\bar{Q}=0$, $\Delta P_\lambda=0$). The variation of the pressure rise ΔP_λ with mean flux $\bar{Q}$ is calculated from Eq. (60) and drawn in Fig. 2. at different parameters values. Figs. 2(a) and (2b) illustrate the pressure rise of the Carreau fluid (n=0.398) and Newtonian fluid (n=1) for various values of the partial slip parameter β. It is shown in Fig. 2(a), that there is an inversely nonlinear relation between the pressure rise ΔP_λ and the time mean volume flow rate $\bar{Q}$, i.e. the pressure rise decreases with increasing the

partial slip parameter β in peristaltic pumping region ($\bar{Q}$>0, ΔP_λ>0). Also, the behavior of the Newtonian fluid (linear, n=1) is as Carreau fluid in peristaltic pumping region ($\bar{Q}$>0, ΔP_λ>0). Figs. 2(c) and 2(d) represents the several values of Weissenberg number (We < 1) for pressure rise with volume flow rate, where it is observed that there is a Nonlinear relation in Carreau fluid and a linear relation in Newtonian fluid and the pressure rise increases with increasing Weissenberg number We in peristaltic pumping region ($\bar{Q}$>0, ΔP_λ>0) for both fluids [Carreau (n=0.398) and Newtonian fluid (n=1)]. Also we found that the pumping curves are intersecting at retrograde pumping region ($\bar{Q}$<0, ΔP_λ>0) for Carreau fluid and the pumping curves are intersecting at copumping region ($\bar{Q}$>0, ΔP_λ<0). It is observed that the pressure rise decreases with increasing the amplitude ratio Φ in the peristaltic pumping region ($\bar{Q}$>0, ΔP_λ>0) and the pumping curves are coinciding in the copumping region ($\bar{Q}$>0, ΔP_λ<0) from Fig. 2(e). Fig. 2(f) shows a comparison of the Carreau fluid and Newtonian fluid; it is observed that the pumping curves are intersecting in the peristaltic pumping region ($\bar{Q}$>0, ΔP_λ>0), it is also found that the pressure rise decrease with increasing Carreau fluid (n=0.398, 0. 498) to Newtonian fluid (n=1) in retrograde pumping region ($\bar{Q}$<0, ΔP_λ>0). However, the curves for Carreau fluid tend to approach the curve for the Newtonian fluid as n→1 and opposite behavior in copumping region ($\bar{Q}$>0, ΔP_λ<0).

The velocity profiles for different values of volume flow rate, partial slip parameter β and Weissenberg number are discussed in Fig. 3. It is observed from Fig. 3(a) that the velocity profiles increases with increase volume flow rate. Fig. 3(b) shows the influence of the partial slip parameter β on the axial velocity, it is found that the magnitude of the axial velocity decreases in the center and increases nearer at the walls of the channel with increasing partial slip parameter β. Fig. 3(b) shows the effect of the Weissenberg number We on the magnitudes of the velocity, it is observed that the profiles decrease with increasing Weissenberg number We. It is also observed in Fig. 3(d) that the velocity deceases from Carreau fluid (n=0.398, 0.498) to Newtonian fluid (n=1). Fig. 4 is plotted to see the effect of the parameters $\bar{Q}$, β, and We on the pressure gradient dp/dx. Figs. 4(a)-4(c) show that the pressure gradient dp/dx decreases with increasing the volume flow rate, partial slip parameter β and Weissenberg number We. Fig. 4(d) indicates that the pressure gradient increases from Carreau fluid (n=0.398, 0.498) to Newtonian fluid (n=1). The variation of the axial shear stress τ_{xy} with y is calculated from Eq. (61) and is shown in Fig.5 for different physical parameters. In Figs. 5(a) and 5(c) we observe that the curves intersect at origin and the axial shear stress τ_{xy} increases with increasing the volume flow and Weissenberg number We in the upper wall and an opposite behavior is observed in the lower wall of the channel. The relation between the shear stress τ_{xy} and y at different values the partial slip parameter β is depicted in Fig. 5 (b). We observe that the curves intersect at the origin and the shear stress τ_{xy} decreases with increasing the partial slip parameter β above the origin while an opposite behavior is observed below the origin and no effect at the walls. It is observed from Fig. 5(d) that the shear stress τ_{xy} decreases from Carreau fluid (n=0.398, 0.498) to Newtonian fluid (n=1).

Trapping phenomena

Another interesting phenomenon in peristaltic motion is the trapping. It is basically the formation of an internally circulating bolus of fluid by closed stream lines. The trapped bolus will be pushed ahead along the peristaltic waves. The stream lines are calculated form Eq. (57) and plotted in Figs. 6-10. Fig. 6 shows the effects of the amplitude ratio Φ on the stream lines, it is found that the bolus moves from the central region towards left and decrease with increasing the amplitude ratio Φ. It is shown in Fig. 7 that the size of bolus increases with increasing the volume flow rate while the bolus disappears for $\bar{Q}$=0.5. Fig.8 is depicted for various values of the partial slip parameter β, It is found that the volume of the trapping bolus decreases as the partial slip parameter β increases, moreover, the bolus disappear at β=0.06. The stream lines are drawn in Fig.9 for different values of Weissenberg number We, it is found that the size of the trapping bolus increases with as Weissenberg number We increases. Figs. 9-10 compare for different wave forms like sinusoidal wave, triangular wave, trapezoidal wave, square wave and sawtooth wave, it is finally observed that the volume of trapping bolus increases from Carreau fluid(n=0.398) to Newtonian fluid(n=1).

VII. CONCLUSION

In the present note, we have discussed the peristaltic motion of a Carreau fluid in an asymmetric channel with partial slip β. The two-dimensional governing equations have been modeled and then simplified using the long wave length approximation and then solved by using the perturbation technique. The results are discussed through graphs. We have concluded the following observations:

- The magnitude of the velocity field increases near the walls and decreases at the center of the channel with increasing the partial slip parameter β.
- The pressure gradient decreases with increasing the partial slip parameter β, Weissenberg number We and the volume flow rate$\bar{Q}$.
- In the peristaltic pumping region the pressure rise increases with increasing Weissenberg number We and decreases as the partial slip parameter β increases.
- The shear stress distribution increases in the upper wall and decreases in the lower wall with decreasing β and decreasing Weissenberg We.
- The size of tapping bolus decreases with increasing the partial slip β while it disappears at β=0.06.
- The size of the trapping bolus increases from Carreau fluid (n=0.398) to Newtonian fluid (n=1).

APPENDIX: EXPRESSIONS FOR WAVE SHAPES

The non-dimensional expressions for the five considered wave forms are given by the following equations:

I. Sinusoidal wave:

$$h_1(x) = 1 + a\sin(x), \tag{A.1}$$

$$h_2(x) = -d - b\sin(x + \phi), \tag{A.2}$$

II. Triangular wave:

$$h_1(x) = 1 + a\left\{\frac{8}{\pi^3}\sum_{m=1}^{\infty}\frac{(-1)^{m+1}}{(2m-1)^2}\sin[(2m-1)x]\right\}, \tag{A.3}$$

$$h_2(x) = -d - b\left\{\frac{8}{\pi^3}\sum_{m=1}^{\infty}\frac{(-1)^{m+1}}{(2m-1)^2}\sin[(2m-1)x + \phi]\right\}, \tag{A.4}$$

III. Square wave:

$$h_1(x) = 1 + a\left\{\frac{4}{\pi}\sum_{m=1}^{\infty}\frac{(-1)^{m+1}}{(2m-1)}\cos[(2m-1)x]\right\}, \tag{A.5}$$

$$h_2(x) = -d - b\left\{\frac{4}{\pi}\sum_{m=1}^{\infty}\frac{(-1)^{m+1}}{(2m-1)}\cos[(2m-1)x + \phi]\right\}, \tag{A.6}$$

IV. Trapezoidal wave:

$$h_1(x) = 1 + a\left\{\frac{32}{\pi^2}\sum_{m=1}^{\infty}\frac{\sin\frac{\pi}{8}(2m-1)}{(2m-1)^2}\sin[(2m-1)x]\right\}, \tag{A.7}$$

$$h_2(x) = -d - b\left\{\frac{32}{\pi^2}\sum_{m=1}^{\infty}\frac{\sin\frac{\pi}{8}(2m-1)}{(2m-1)^2}\sin[(2m-1)x + \phi]\right\}. \tag{A.8}$$

V. Sawtooth wave:

$$h_1(x) = 1 + a\left\{\frac{8}{\pi^3}\sum_{m=1}^{\infty}\frac{\sin[2m\pi x]}{m}\right\}, \tag{A.9}$$

$$h_2(x) = -d - b\left\{\frac{8}{\pi^3}\sum_{m=1}^{\infty}\frac{\sin[2m\pi x]}{m} + \phi\right\}. \tag{A.10}$$

REFERENCES

[1] O. Eytan, AJ. Jaffa, Har-toov, J. Dalach, E. Elad, Dynamic of the intrauterine fluid-wall interface, Ann Biomed Eng, **27**(1999) 372-379

[2] O. Eytan, D. Elad, Analysis of Intra-uterine fluid motion induced uterine contractions. Bull math Biol. 61(1999), 221-238.

[3] M. Mishra, A. Ramachandra Rao, Peristaltic transport of a Newtonian fluid in an asymmetric channel, Z. Angew. Math. Phys. 54(2004), 532-550.

[4] M. Mishra, A. Ramachandra Rao, Nonlinear and curvature effects on peristaltic flow of a viscous fluid in an asymmetric channel, Acta Mechanica, 168(2004), 35-39.

[5] T. Hayat, Nasir Ali, Zaheer Abbas**,** Peristaltic flow of a mocropolar fluid in a channel with different wave forms, Phys. Lett. A, 370 (2008), 331-344.

[6] K. Vajravelu, S. Sreenadh. R. Hemadri Reddy, K. Murugesan, Peristaltic transport of a Casson fluid in contact with a Newtonian **f**luid in a circular **t**ube with permeable wall, Int. Journal of Fluid Mechanics Research, Vol. 36(2009)(3), 244-254.

[7] Nasir Ali, T. Hayat, Peristaltic motion of a Carreau fluid in an asymmetric channel, Applied Mathematics and computation 193(2007), 535-552.

[8] K. Vajravelu, S. Sreenadh, K. Rajanikanth, Chanhoon Lee, Peristaltic transport of a Williamson fluid in asymmetric channels with permeable walls, Nonlinear Analysis: Real World Applications 13(2012) , 2804-2822.

[9] S. Nadeem, Safia Akram, Heat transfer in a peristaltic flow of MHD fluid with partial slip, Commun Nonlinear Sci Numer Simulat 15(2010), 312–321.

[10] T. Hyat, Q. Hussain, N.Ali, Influence of the partial slip on the peristaltic flow in a porous medium, Physica A 387 (2008) 3399–3409.

[11] Prasana Hariharan, V. Seshadri, Rupak K. Banerjee, Peristaltic transport of non-Newtonian fluid in a diverging tube with different wave forms, Mathematical and Computer Modeling**,** 48(2008) 998-1017.

[12] M.V.Subba Reddy, A. Ramachandra Rao, S. Sreenadh, Peristaltic motion of a power-law fluid in an asymmetric channel, Int. J. Non-Linear Mech. 42(2007) 1153-1161.

[13] A. Ebaid, Effects of magnetic field and wall slip condition on the peristaltic transport of a Newtonian fluid in asymmetric channel, Physics letters A 372(2008) 4493-4499.

[14] S. Srinivas, M. Kothandapani, The influence of heat and mass transfer of MHD peristaltic flow through a porous space with complaints walls, Applied Mathematics and Computation 213 (2009) 197- 208.

[15] S. Nadeem, S. Akram, Heat transfer in a peristaltic flow of MHD fluid with partial slip, Communications in Nonlinear Science and Numerical Simulation 15 (2010) 312 - 321

[16] R.B. Bird, R.C. Armstrong, O. Hassager, Dynamics of Polymeric Liquids, vol. 1, Wiley, New York, 1977:

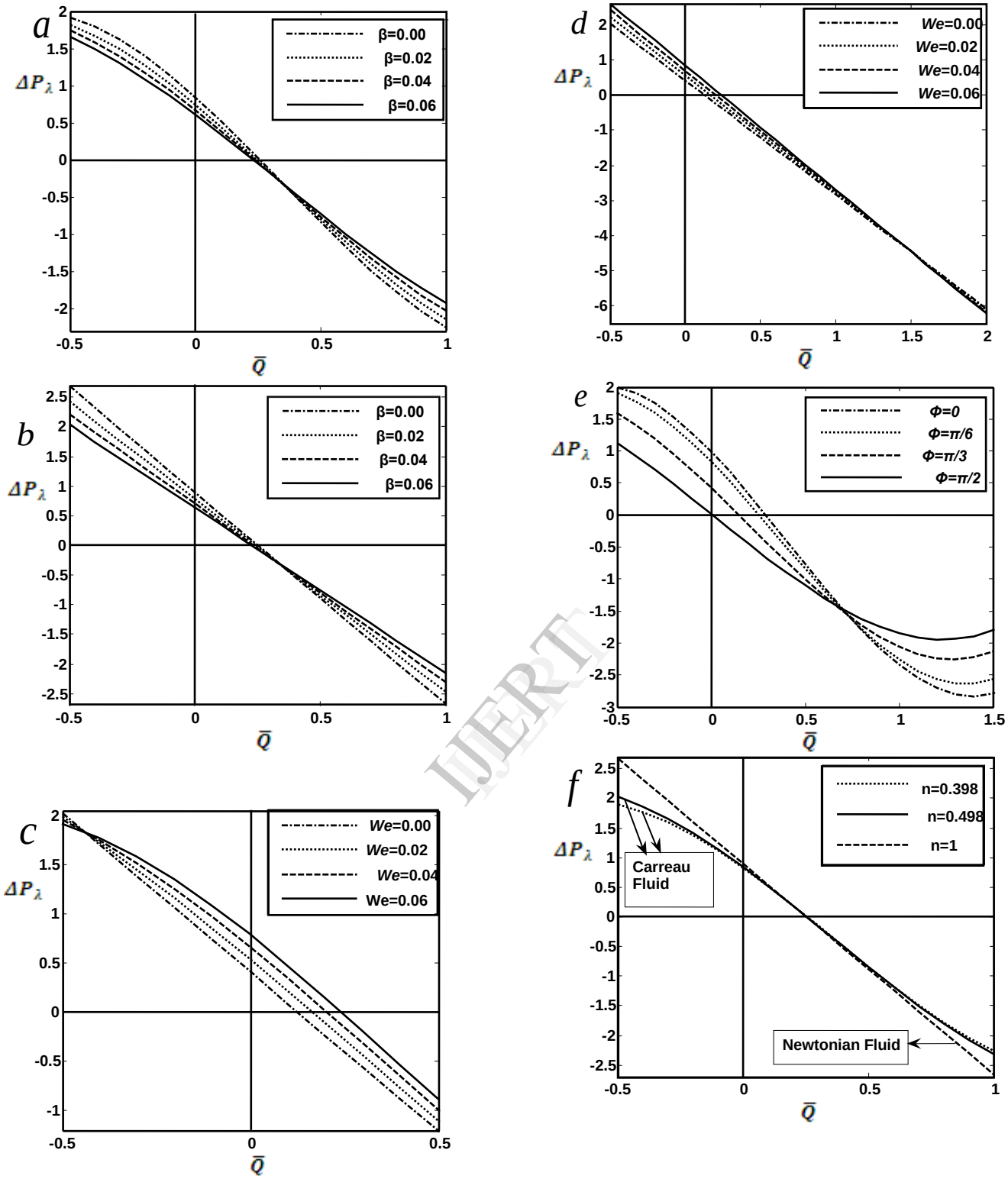

Fig. 2: Variation of $\bar{Q}$ with ΔP_λ for a=0.5, b=0.5, d=1; (a) Φ=π/6, n=0.398, We=0.01; (b) Φ=π/6, n=1, We=0.01; (c) Φ=π/6, n=0.398, β=0.01; (d) Φ=π/6, n=1, β=0.01; (e) n=.398, We=0.01, β=0.01; (f) Φ=π/6, β=0.01, We=0.01.

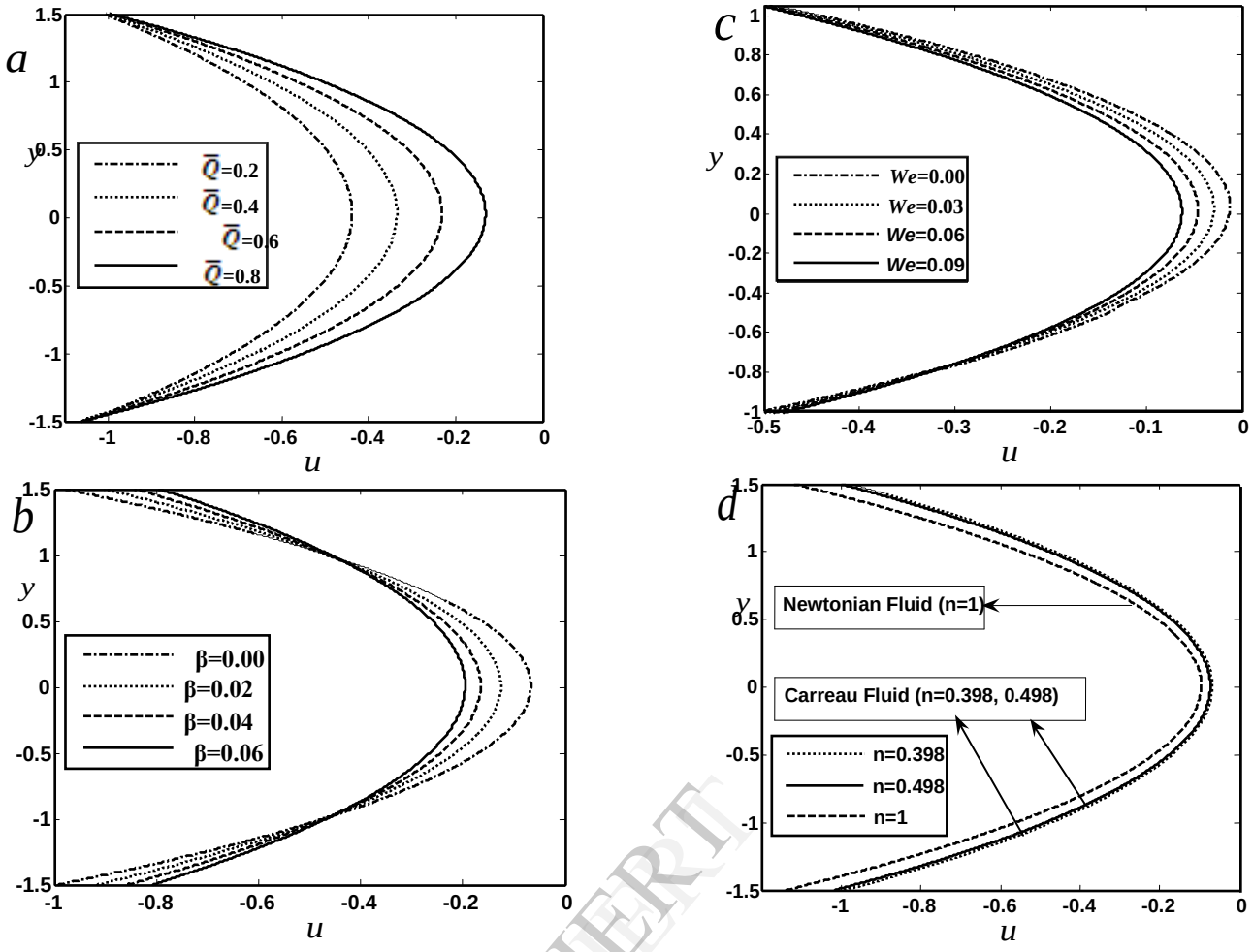

Fig. 3: The velocity profiles for a=0.5, b=0.5, d=1.25, x=1, $\Phi=\pi/6$; (a) β=0.01, n=0.398, We=0.01; (b) $\bar{Q}$=1, n=0.398,We=0.01; (c) $\bar{Q}$=1, β=0.01, n=0.398; (d)) $\bar{Q}$=1, β=0.01, We=0.01.

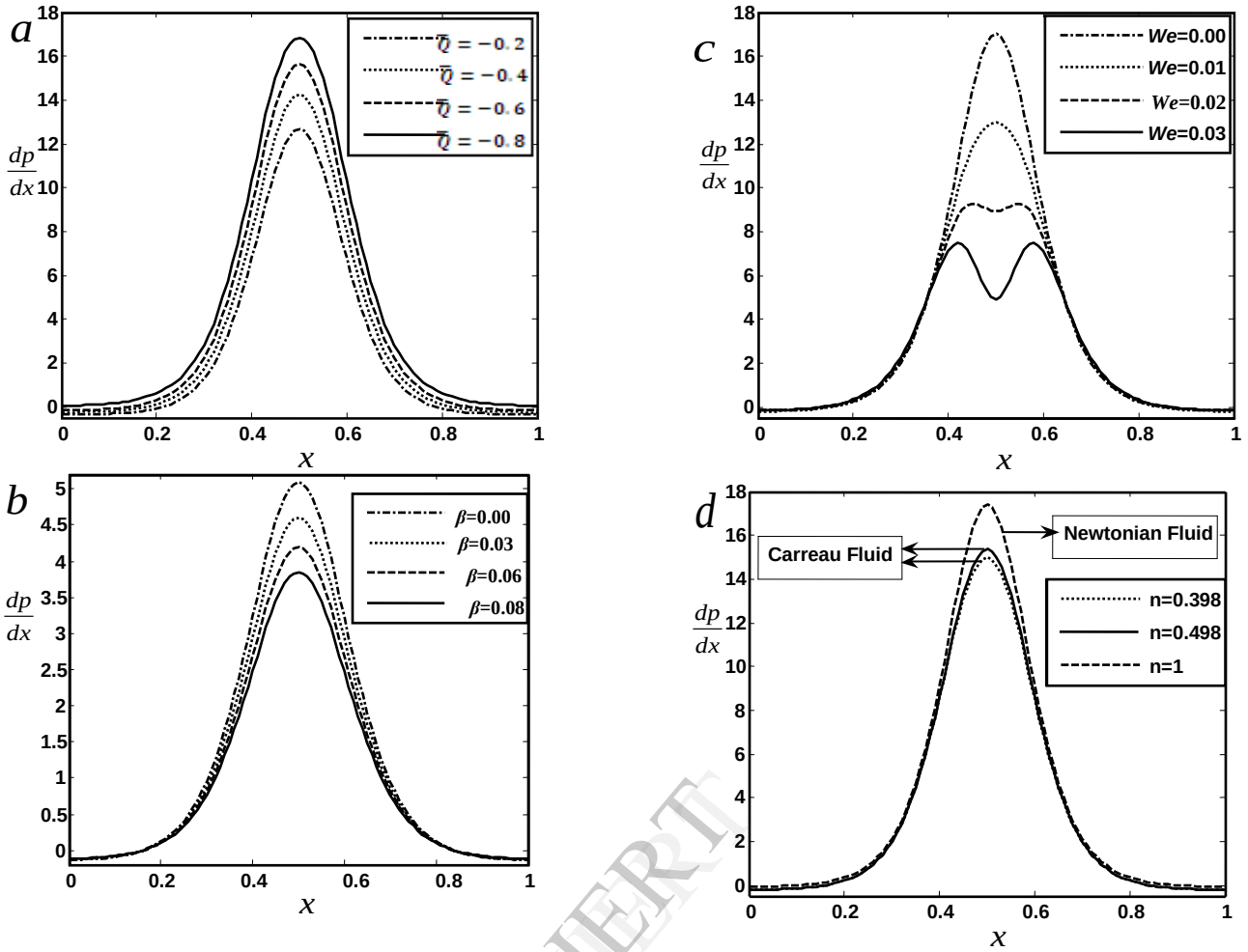

Fig. 4: Pressure distribution for a=0.5, b=0.5, d=1.25, Φ=0; (a) n=0.398, β=0.01, We =0.01; (b) $\bar{Q}$=-1, n=0.398, We=0.01; (c) $\bar{Q}$=-1, n=0.398, β=0.01; (d) $\bar{Q}$=-1, β=0.01, We=0.01

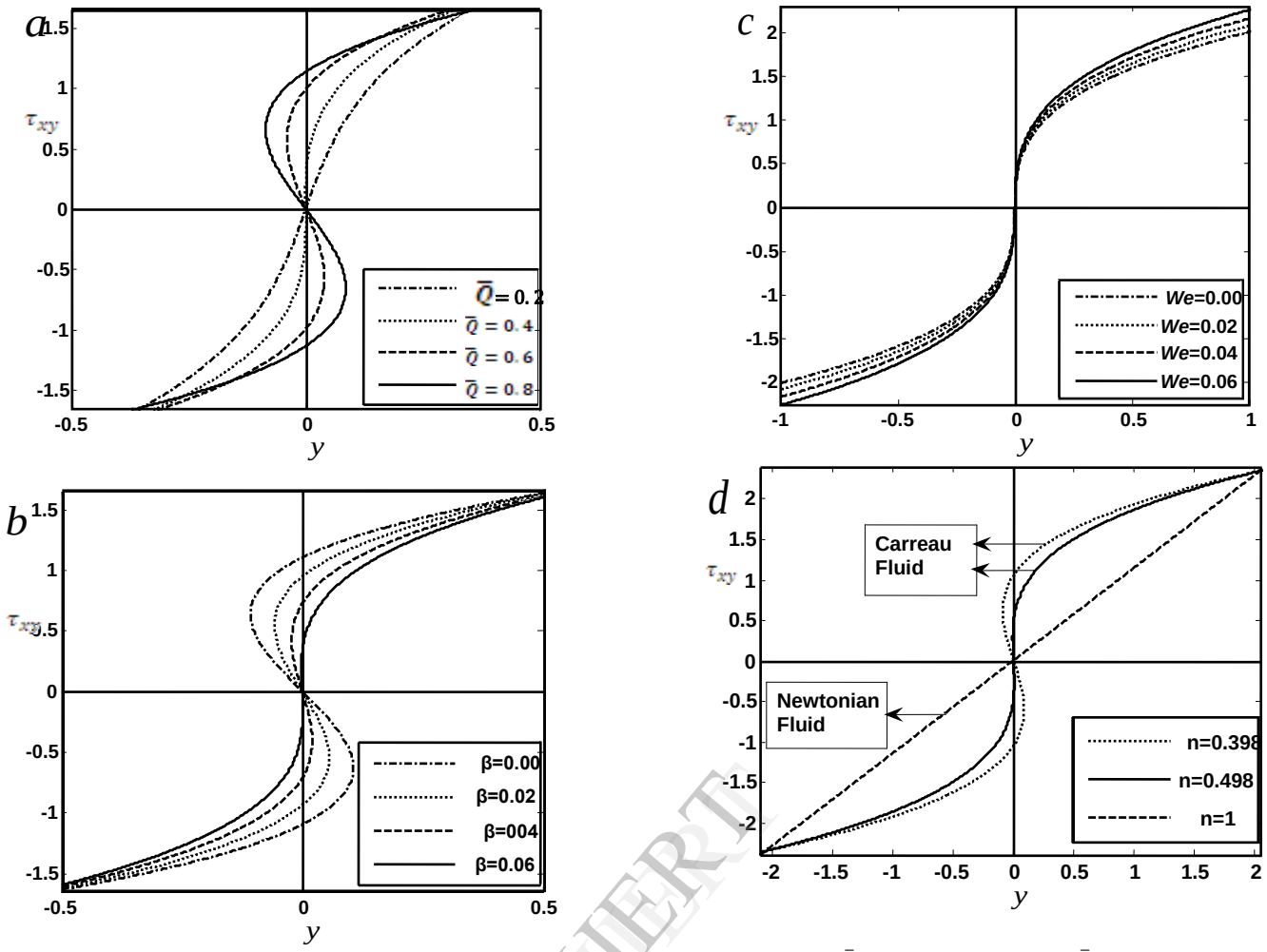

Fig. 5: The axial shear stress distributions τ_{xy} with y for a=0.5, b=0.5, d=1, Φ=π/6; (a) $\bar{Q}$=1, We=0.01, n=0.398; (b) $\bar{Q}$=1, β=0.01, n=0.398;(c) $\bar{Q}$=1, β=0.01, n=0.398; (d) We = 0.01, β=0.01, $\bar{Q}$=1.

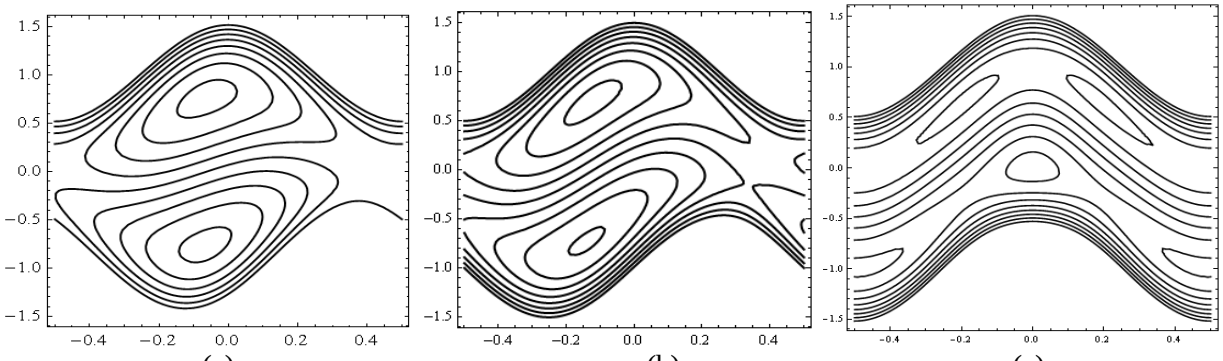

Fig. 6: Stream lines for different values of mean flow rate a=0.5, b=0.5, d=1, $\bar{Q}$=1.6. Φ=0, n=0.398, We = 0.01, β=0.01; (a) Φ=π/6; b) Φ=π/3; (c) Φ=π/2.

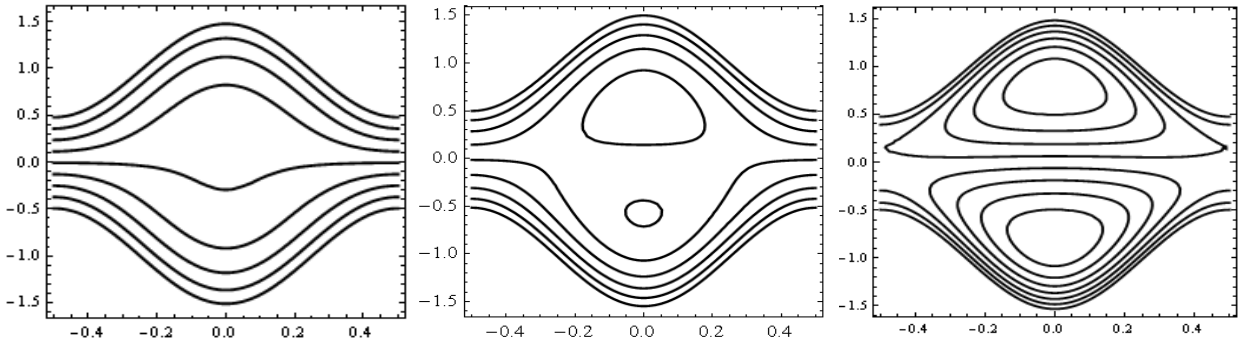

(a) (b) (c)

Fig. 7: Stream lines for different values of mean flow rate a=0.5, b=0.5, d=1, Φ=0, n=0.398, $We = 0.01$; (a) $\bar{Q}$=0.5, (b) $\bar{Q}$=1; (c) $\bar{Q}$=1.5.

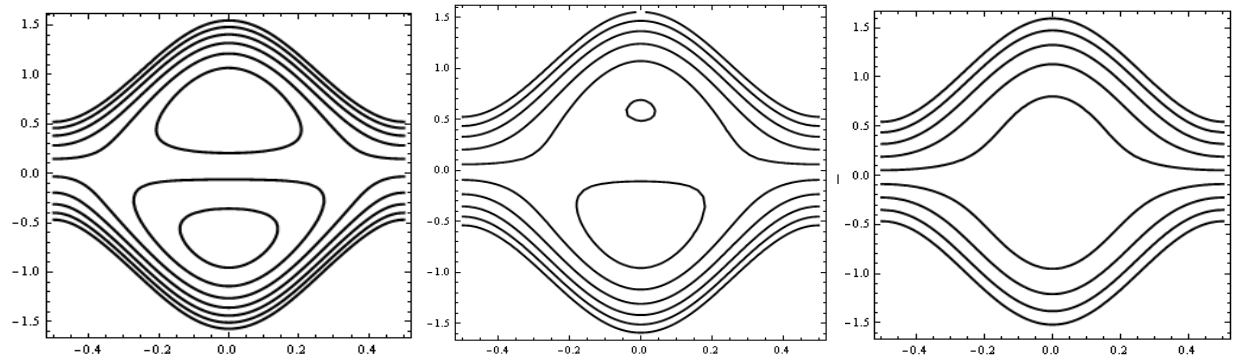

(a) (b). (c)

Fig. 8: Stream lines for different values of mean flow rate a=0.5, b=0.5, d=1, Φ=0, n=0.398, $We = 0.01$, $\bar{Q}$=1; (a)β=0.00; (b)β=0.02; (c) β=0.06.

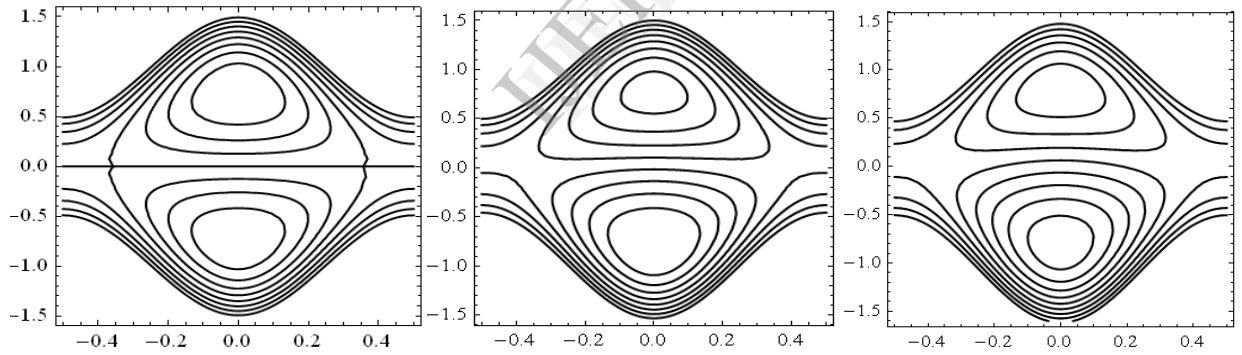

(a) (b) (c)

Fig. 9: Stream lines for different values of mean flow rate a=0.5, b=0.5, d=1, Φ=0, n=0.398, $\beta = 0.01$, $\bar{Q}$=1; (a) We=0.00; (b) We=0.04; (c)We=0.08.

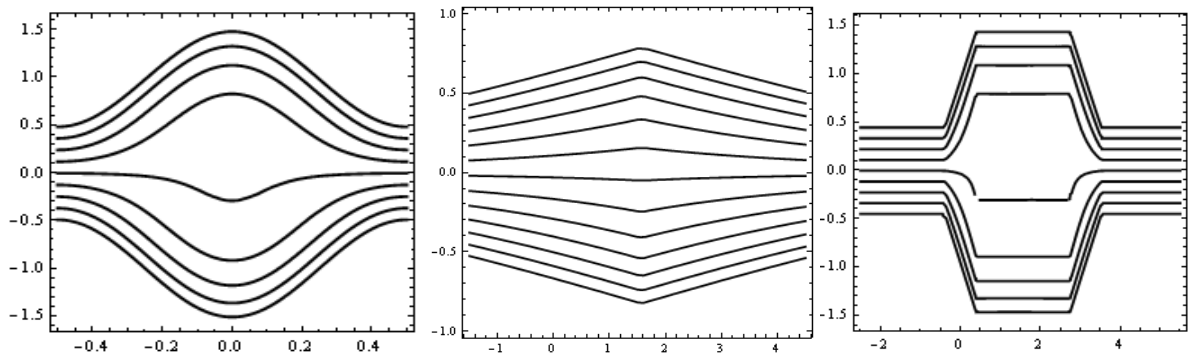

(a) (b). (c)

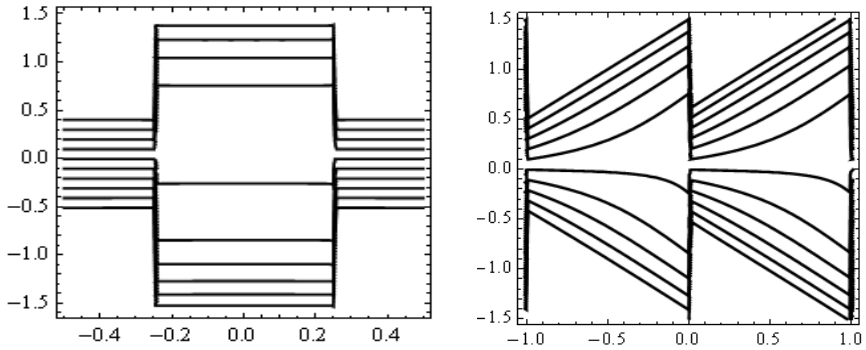

(d) (e)

Fig. 10: Stream lines for five different wave forms of Carreau fluid (n=0.398) (a) sinusoidal wave, (b) triangular wave (c) trapezoidal wave (d) square wave (e) sawtooth wave with a=0.5, b=0.5, d=1, Φ=0, $\bar{Q}$=1, β=0.01 and We =0.01.

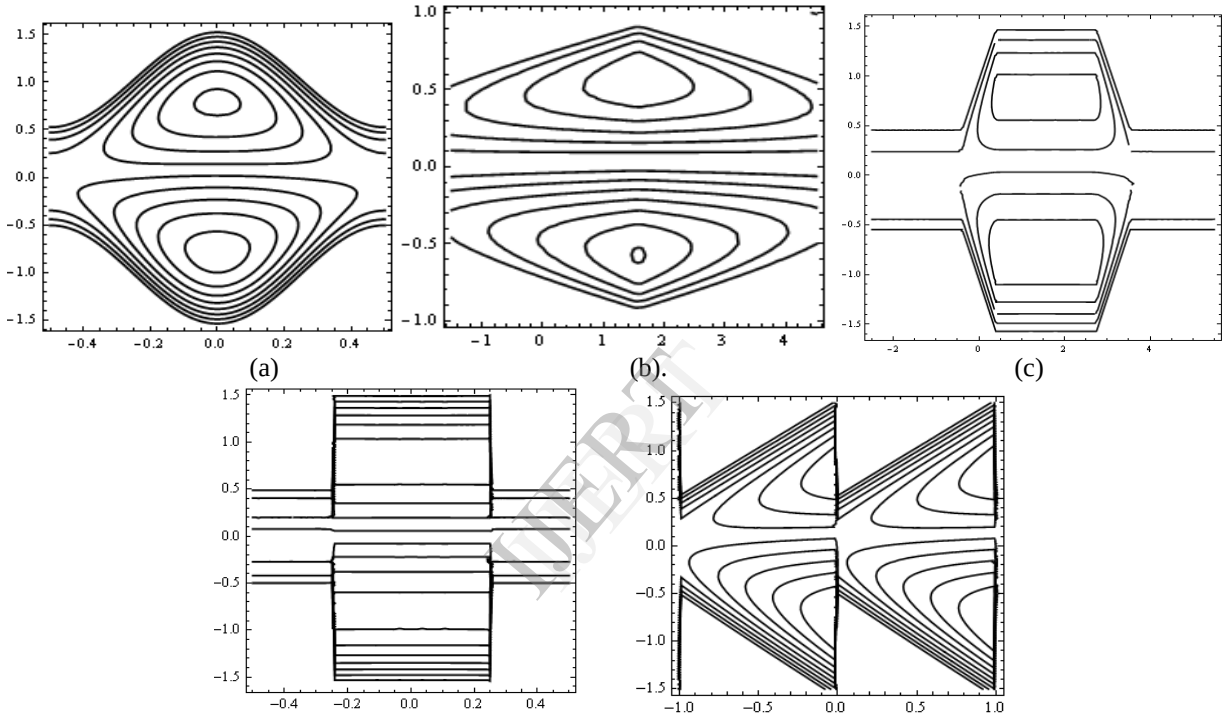

(a) (b). (c)

(d) (e)

Fig. 11: Stream lines for five different wave forms of Newtonian fluid(n=1); (a) sinusoidal wave; (b) triangular wave; (c) trapezoidal wave; (d) square wave; (e) sawtooth wave with a=0.5, b=0.5, d=1, Φ=0, $\bar{Q}$=1, β=0.01 and *We* =0.01.